Environment Setup and Model Benchmark of the MuFoRa Dataset

Islam Fadl[1], Torsten Schön[3], Valentino Behret[2], Thomas Brandmeier[1], Frank Palme[2] and Thomas Helmer[1]

[1]*CARISSMA Institute of Safety in Future Mobility (C-ISAFE), Technische Hochschule Ingolstadt, Esplanade 10, Ingolstadt, Germany*

[2]*Laboratory for 3D Measuring Systems and Computer Vision, Department of Mechanical, Automotive and Aeronautical Engineering, Munich University of Applied Sciences (MUAS), Dachauer Straße 98b, Munich, Germany*

[3]*AIMotion Bavaria, Technische Hochschule Ingolstadt, Ingolstadt, Germany*

Islam.Fadl@carissma.eu, {Valentino.Behret, Frank.Palme}@hm.edu,

Keywords: Dataset, Multimodal, Benchmark, Adverse Weather, Computer Vision, Perception.

Abstract: Adverse meteorological conditions, particularly fog and rain, present significant challenges to computer vision algorithms and autonomous systems. This work presents MuFoRa[a] a novel, controllable, and measured multimodal dataset recorded at CARISSMA's indoor test facility, specifically designed to assess perceptual difficulties in foggy and rainy environments. The dataset bridges research gap in the public benchmarking datasets, where quantifiable weather parameters are lacking. The proposed dataset comprises synchronized data from two sensor modalities: RGB stereo cameras and LiDAR sensors, captured under varying intensities of fog and rain. The dataset incorporates synchronized meteorological annotations, such as visibility through fog and precipitation levels of rain, and the study contributes a detailed explanation of the diverse weather effects observed during data collection in the methods section. The dataset's utility is demonstrated through a baseline evaluation example, assessing the performance degradation of state-of-the-art YOLO11 and DETR 2D object detection algorithms under controlled and quantifiable adverse weather conditions. The public release of the dataset[b] facilitates various benchmarking and quantitative assessments of advanced multimodal computer vision and deep learning models under the challenging conditions of fog and rain.

[a]**MuFoRa** – A **Mu**ltimodal Dataset of Traffic Elements Under Controllable and Measured Conditions of **Fo**g and **Ra**in

[b]https://doi.org/10.5281/zenodo.14175611

1 INTRODUCTION

Autonomous vehicles rely on perception systems, including radars, cameras, and LiDARs, for (critical) driving decisions. However, real-world driving scenarios present unmeasured and uncontrolled amounts of rain and fog, creating ambiguity in algorithm performance under adverse weather conditions. To address this challenge, the BARCS project aims to develop a safe operator-free shuttle bus for last-mile transport in rural areas. To assess perception system limitations in adverse weather, the project utilizes the CARISSMA-THI indoor test facility in Ingolstadt, Germany (Vriesman et al., 2020), (Sezgin et al., 2023), where cameras and LiDARs are tested under measurable, controllable, reproducible and realistic rain and fog conditions (Graf et al., 2023). This well-defined environment allows for the creation of a benchmark dataset, crucial for evaluating object detection models and other perception algorithms, which clearly defines its limitations in adverse weather conditions.

This study evaluates the performance of state-of-the-art object detection models across dry, rainy, and foggy conditions. To facilitate this research, a multimodal dataset is publicly released comprising synchronized, rectified, and calibrated RGB images and point clouds (Behret et al., 2025). The data were captured at incremental distances (5 - 50 meters) between traffic elements and vehicle-mounted sensors, allowing for comprehensive analysis. The dataset enables researchers to assess the specific distortions and hindrances affecting individual sensor modalities, particularly cameras and LiDARs, in adverse weather. The

Fadl, I., Schön, T., Behret, V., Brandmeier, T., Palme, F. and Helmer, T.
Environment Setup and Model Benchmark of the MuFoRa Dataset.
DOI: 10.5220/0013307900003912

In *Proceedings of the 20th International Joint Conference on Computer Vision, Imaging and Computer Graphics Theory and Applications (VISIGRAPP 2025) - Volume 3: VISAPP*, pages 729-737
ISBN: 978-989-758-728-3; ISSN: 2184-4321

work focuses on two main objectives:

(1) Creating and releasing a novel multimodal benchmarking dataset for researching adverse weather conditions implications on autonomous driving perception algorithms, in controllable and measurable environments and their corresponding annotations at a sequence-level.

(2) Evaluating state-of-the-art object detection models with 2D images in various fog and rain conditions, i.e. when visibility is approximately 10, 30, and 100 meters during foggy conditions, and at rain precipitation of 20, 40, 60, 80, and 100 mm/h.

By addressing these aspects, this research contributes to developing a more robust evaluation methodology of perception systems in autonomous vehicles, enhancing their performance across various weather conditions.

2 RELATED WORK

The development of robust autonomous driving systems that can operate effectively in adverse weather conditions remains a significant challenge in the field (Jokela et al., 2019). Although numerous datasets have been released in recent years to tackle this issue, a comprehensive dataset with measured weather parameters is still lacking. This literature review explores the current landscape of datasets used for benchmarking and advancing autonomous driving systems, with a specific focus on those designed to address challenging weather conditions such as fog and rain.

Several large-scale datasets have been instrumental in advancing autonomous driving research. The Waymo Open Dataset (Sun et al., 2020) provides a comprehensive collection of sensor data from urban and suburban environments, including some adverse weather scenarios. Similarly, the KITTI dataset (Geiger et al., 2013) offers a diverse range of urban and rural scenes, while the more recent KITTI-360 (Liao et al., 2022) expands on this with 360-degree views. The nuScenes dataset (Caesar et al., 2020) provides multimodal sensor data from urban environments in Boston and Singapore, including various weather conditions.

However, these datasets, while valuable, do not offer controllable and measurable adverse weather conditions, limiting their utility for systematic evaluation of autonomous driving systems in challenging environments. This gap has led to the development of specialized datasets focusing on adverse weather.

DAWN (Detection in Adverse Weather Nature) (Kenk and Hassaballah, 2020) and SID (Stereo Image Dataset) (El-Shair et al., 2024) datasets specifically address vehicle detection in diverse traffic environments (urban, highway and freeway) with adverse weather, including fog, snow, rain, and sandstorms. Similarly, datasets like ONCE (Mao et al., 2021), and BDD100K (Yu et al., 2020) offer valuable real-world scenarios, but their lack of control over weather conditions limits their effectiveness for a measurable evaluation in adverse weather.

Synthetic datasets have emerged as an alternative to the need for diverse and adverse weather conditions. Datasets like SYNTHIA (Ros et al., 2016) offer various weather scenarios with synthetic data. RainyCityscapes (Hu et al., 2019) stand out for synthetic rain removal added to the original Cityscapes (Cordts et al., 2016). WEDGE dataset (Marathe et al., 2023) uses generative vision-language models to create a multi-weather autonomous driving dataset, offering 16 extreme weather conditions. This approach allows for more control over weather conditions but may not fully provide quantifiable weather effects, besides the challenge of bridging the simulation-reality gap resulting from synthetic dataset usage (Hu et al., 2019).

Recent research has highlighted the importance of multimodal approaches in adverse weather. (Bijelic et al., 2020) demonstrated the effectiveness of deep multimodal sensor fusion in fog conditions, emphasizing the need for datasets that include multiple sensor modalities. The SMART-Rain dataset (Zhang et al., 2023) provides a degradation evaluation dataset specifically for autonomous driving in rain.

The impact of adverse weather on different sensor types has been a subject of significant research, (Sezgin et al., 2023) discussed the challenges in object detection under rainy and low light conditions, while (Heinzler et al., 2019) examined weather influence on automotive LiDAR sensors. (Jokela et al., 2019) conducted testing and validation focusing on automotive LiDAR sensors in fog and snow.

Recent trends in the field include the exploration of radar as a potential replacement for LiDAR in all-weather mapping and localization (Burnett et al., 2023), and the development of voxel-based 3D object detection methods (Deng et al., 2021) (Deng et al., 2021) (Zhou and Tuzel, 2017) which may be more robust to adverse weather conditions.

While datasets such as ONCE (Mao et al., 2021), BDD100K (Yu et al., 2020), and ACDC (Sakaridis et al., 2021) offer valuable real-world scenarios, their lack of control over weather conditions limits their effectiveness for specific, measurable evaluations.

Despite advancements, there is still a lack of datasets with controllable and measurable adverse

Table 1: Comparison of datasets focusing on weather effects using different attributes.

Attribute	MuFoRa	WEDGE	DAWN	SID
Modalities	Images and Point Clouds	Images	Images	Images
Place	Indoors	Synthetic (DALL-E)	Urban, Highway	University campus, urban and residential areas
Weather Effects	Fog, Rain, Dry, Dim, Dark	16 Weather Effects	Fog, Snow, Rain, Sandstorms	Clear, Snow, Cloudy, Rain, Overcast
Measured Weather Effects	**Yes**	No	No	No
Sequences / Frames	90 Sequences	3660 Images	1000 Images	27 Sequences

weather conditions, especially for fog and rain. The development of a novel public dataset with controllable fog and rain addresses this gap, offering a valuable tool for benchmarking and improving deep learning models, such as depth estimation and object detection, in measurable adverse weather. This could significantly enhance the safety and reliability of autonomous systems across diverse conditions. To our knowledge, this is the first public multimodal dataset featuring both measured rain precipitation and measurable visibility in foggy conditions, all created in a controlled environment at the CARISSMA-THI indoor test facility. Table 1 presents an overview of datasets focusing on different weather conditions.

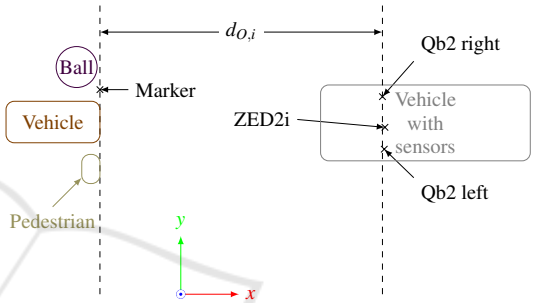

Figure 1: Sensor setup during the calibration process using the total station.

3 METHODS

3.1 Experiment Setup

Data collection is conducted under three weather scenarios to establish various thresholds for computer vision algorithms in adverse weather conditions. Additionally, during each weather condition, three target objects are placed at varying distances from the stereo cameras and LiDARS Figure 1. The scenarios include

(1) Dry conditions with normal, dim light and darkness.

(2) A ramp of fog resulting in a continuous visibility gradient from 8 to 100 meters.

(3) Five precipitation levels of rain.

To generate ground truth data for object detection, the relative positions of the sensors to the objects have to be determined. This can be achieved by calibrating marker positions using a total station. As Figure 1 shows, for each distance $d_{O,i}$ a marker was placed on the ground. These markers are used to determine the distance of the three objects (1) ball, used for calibration, (2) vehicle, and (3) pedestrian in the x-direction from the sensors. In total, ten markers were placed on the ground to cover the distances from 5 m to 50 m with a step size of 5 m.

The sensors and marker positions were calibrated using the total station before starting the data recording. The calibration had to be repeated each recording day since the vehicle with the sensor setup was moved in between the recording days. As Table 4 (see Appendix) shows the sensor positions could be reproduced from one day to another within a tolerance (3σ) of about $\sim$0.05 m in x-direction, $\sim$0.08 m in y-direction, and less than $>$0.01 m in z-direction.

3.2 Dataset Description

Firstly, the images and point clouds are collected for the three target objects in dry conditions with three light settings. The target objects are static at 10 different distances with increments of 5 meters, starting from 5 to 50 meters away from the sensors mounted on the vehicle. Secondly, The same data collection procedure is repeated under rain. At each distance, data is collected under five different precipitation rates of 20, 40, 60, 80, and 100 mm/h. Therefore, 50 unique sequences of rain are generated. Lastly, the

Table 2: MuFoRa dataset summary under different weather conditions.

Weather Condition	Light Setting / Details	Sequences	Images	Point Clouds
Dry	Light	10	813	827
	Dim (headlights)	10	900	900
	Dark	10	900	870
	Total (All Dry Settings)	30	2,613	2,597
Fog	Visibility ramp increases as fog diffuses	10	29,404	17,629
Rain	Five precipitation intensities (20–100 mm/h)	50	3,810	4,518

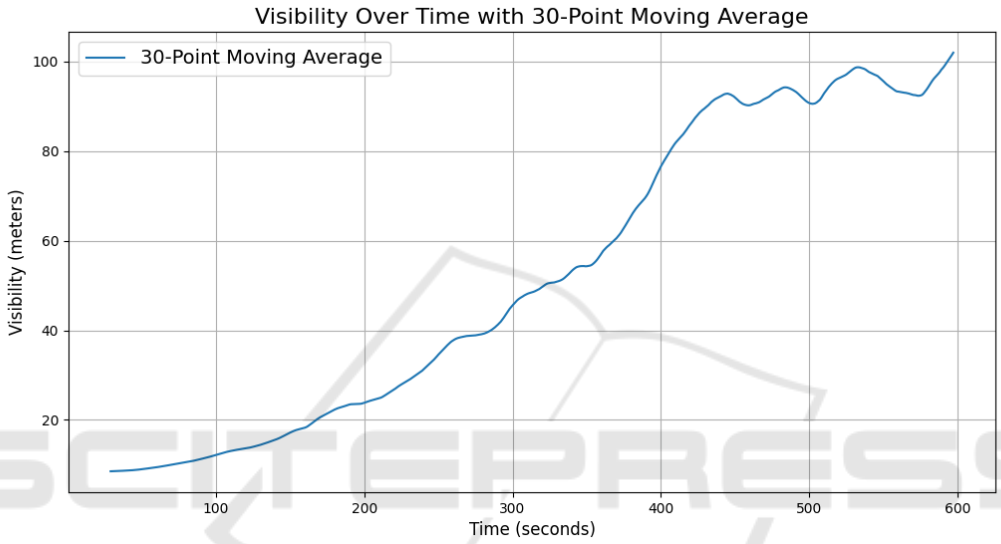

Figure 2: Average visibility across 10 measurements.

hall is saturated with fog until the measured visibility level drops to approximately 8 meters in the hall as shown in Figure 2. The fog gradually dissipates until the measured visibility reaches 100 meters. In this case, the fog data is collected continuously for 10 minutes on average and synchronized with the visibility level allowing for weather-level annotation for the fog-visibility variables, resulting in 10 unique sequences of fog data. Table 2 is an overview of the collected images and point clouds, moreover, Figure 7, Figure 8, Figure 9 and (see Appendix) illustrate the coupled effect on the images collected of distance on one hand, and adverse weather such as rain and fog on the other hand.

The inherent characteristics of fog pose significant challenges in measuring visibility using state-of-the-art devices (Gultepe et al., 2007). Instruments based on obstruction and contamination measurements rely on comparing the scattering and diffusion of emitted and received laser light to determine visibility in foggy environments (Miclea et al., 2020), (Lakra and Avishek, 2022) and (World Meteorological Organization, 2008).

At CARISSMA's indoor test hall facility, VISIC620 is used to measure localized visibility starting from maximum fog density, corresponding to a minimum visibility of approximately 8 meters shown in Figure 8. The fog gradually dissipates, increasing measured visibility as illustrated in Figure 2 until the traffic elements or target objects become humanly visible. Figure 3 shows the visibility curves for each experiment with time stamps, in which the target objects are positioned at a fixed distance from the sensors, during which the fog dissipates gradually.

Visibility measurements fluctuate due to heat dissipation and convection as fog contacts cold surfaces, such as the hall's ground and side walls. This interaction causes the movement of fog layers and variations in fog density, which affect the received laser of the visibility measurement devices ((World Meteorological Organization, 2008), 2008; (SICK AG, 2018)). Therefore, to mitigate these fluctuations, a representative test sample of images or point clouds should span at least 30 consecutive seconds to match the average visibility recorded around the same period, as

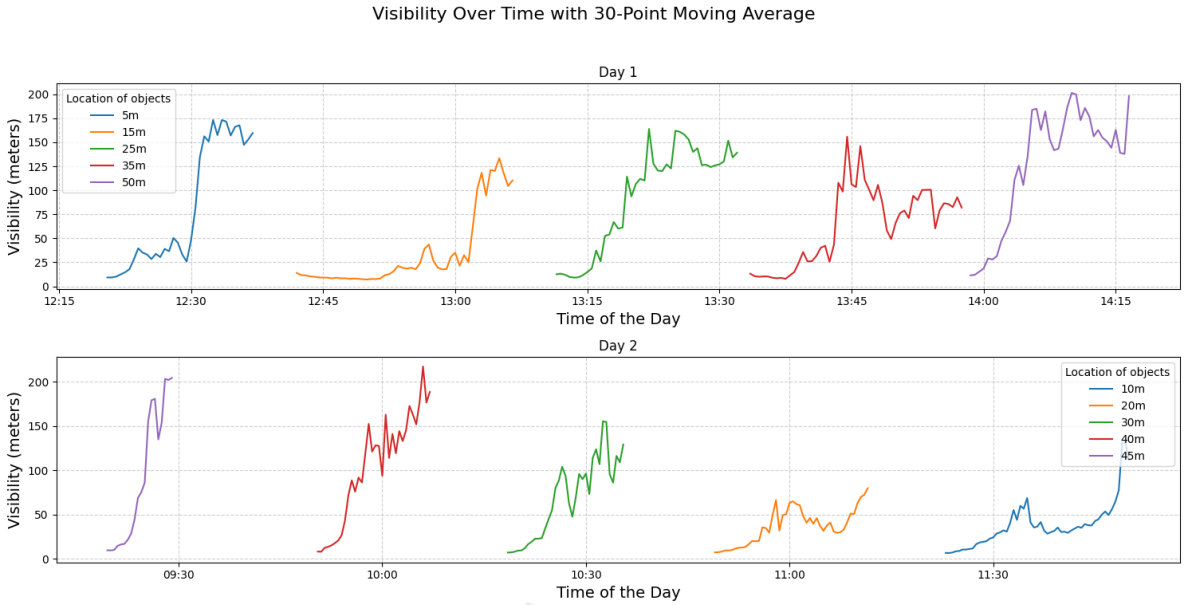

Figure 3: Measured visibility inside CARISSMA's test hall during two days of data collection under fog.

demonstrated in the following evaluation section.

4 EVALUATION

The utility of *MuFoRa* multimodal dataset, which captures target objects under adverse weather conditions and is designed for diverse applications in perception, deep learning, and computer vision research, is demonstrated through an example application. The performance of pre-trained YOLO11x (Jocher et al., 2023) and DETR (backbone R50)(Carion et al., 2020) object detection models are evaluated on sampled images of the dataset using one metric, which is the confidence score.

The evaluation methodology involves two key steps:

Evaluation Dataset. The evaluation sample consists of representative images from dry, rain, and fog conditions with corresponding weather conditions and distance annotations. Since the variations among frames for a given unique sequence under dry and rain conditions are minimal, only 20 images are selected for each unique sequence for evaluation. To conduct a standardized and robust assessment of the model under fog, images must be selected from 30 consecutive seconds or more to overcome fluctuation in visibility measurements as explained in the methods section. The starting distance for fog evaluation is 10 meters, and only 5 distance increments were used 10, 20, 30, 40, and 50 meters, under visibility levels of approximately 10, 30, and 100 meters.

Model Inference. Using the COCO pre-trained YOLO11x and DETR models, the inference is run on the defined test sample of images to generate predictions. The model's outputs predicted bounding boxes, class IDs, and confidence scores. The confidence threshold is set to 0.5. In detection mode, the confidence score for each detected object combines the objectness and class probability scores. The formula is as follows:

$$C = P_{\text{object}} \cdot P_{\text{class}} \tag{1}$$

where: C represents the confidence score for the detected object, P_{object} denotes the objectness score, i.e., the probability that a bounding box contains any object, P_{class} is the probability that the object within the bounding box belongs to a specific class.

This score evaluates the model's certainty that a detected object is present and correctly classified. In this case, a threshold is applied to C to filter out low-confidence detections, which helps reduce false positives.

Figure 4 and Figure 5 shows the confidence score of both models for the *Person* class under dry, three fog, and five rain conditions with several increments of distances. The confidence scores reflect the detection scores of one target object used, i.e. the *4Active* male pedestrian. With both models, the degradation of the confidence score is noticeable after 30 meters. While YOLO results in detections under dry weather conditions at all distances, its degradation of confidence score is more steep. Moreover, YOLO fails to make detections under adverse rain and low visibility at further distances, whereas DETR is more capa-

Table 3: Detection confidence scores of Yolo11x and DETR(R50) for *Person* class under various conditions.

Weather Conditions	Distance (m)	Yolo11 Confidence Score	DETR Confidence Score
Dry	50	0.72	0.97
Rain (100mm/h)	40	-	0.87
Rain (80mm/h)	50	-	0.83
Rain (80mm/h)	40	0.51	0.87
Fog-Visibility (100m)	20	0.84	0.99
Fog-Visibility (30m)	10	0.89	0.99
Fog-Visibility (10m)	10	0.83	0.98

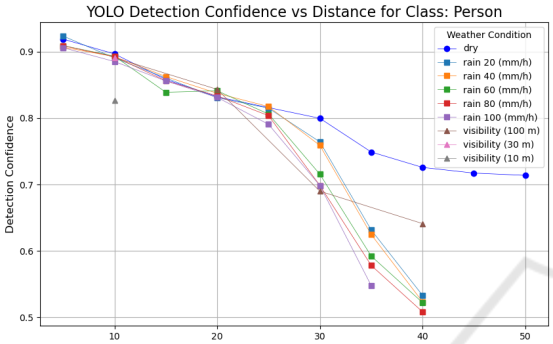

Figure 4: YOLO11x confidence score for the *Person* class under variations of fog, rain, and dry weather.

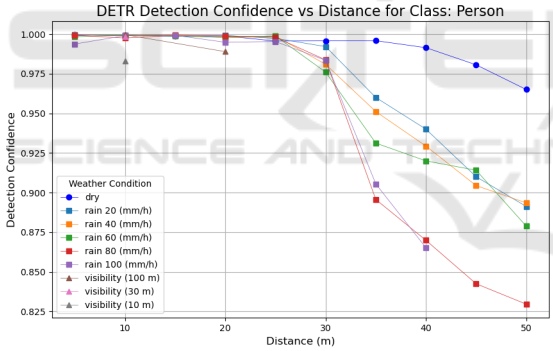

Figure 5: DETR(R50) confidence score for the *Person* class under variations of fog, rain, and dry weather.

ble especially under heavy rain precipitation at further distances above 40 meters. This could be due to the global attention mechanism of DETR. A summary of the confidence scores of both models under severe conditions is shown in Table 3.

The degradation of the confidence score is gradual under dry conditions, where the only variable changing is the location of the objects. While in fog and rain, the challenge is coupled with the image-data quality degradation. The challenge in detection under the rain intensities used starts to be visible at 30 meters and the effect of the distance coupled with rain noise starts to hinder the model's confidence significantly. Furthermore, reflections on the ground surface due to rain as shown, for instance, in Figure 6

Figure 6: Reflection of the ground surface due to rain.

could reduce the confidence scores for other classes e.g. *Car*. While under fog, the score highly depends on the visibility level.

5 CONCLUSIONS

90 novel sequences of controllable and measurable weather scenarios are collected and published, including fog, rain, dry, dark, and dim light conditions. Furthermore, state-of-the-art object detection models are evaluated and critically compared with this unique public dataset in various adverse weather conditions. An illustration of each object detection model's limitation under adverse weather is defined accordingly. An illustration of each object detection model's limitation under adverse weather is defined accordingly, for a more comprehensive evaluation for each model, more metrics should be used.

Future research could focus on collecting dynamic datasets with finer increments of rain, fog, and varying sensor-object distances, in addition to expanding the datasets to include cyclists, groups of people, and strollers. Another approach includes collecting data in challenging constellations where the sensor input would be used for decision-making in autonomous driving in outdoor infrastructure. Furthermore, Identifying real-world gaps, such as the absence of wind and dust in the test hall, and addressing these limitations while evaluating indoor versus real-world data could enhance reliability. Further work could explore challenging driving conditions like headlight reflec-

tions, diffusion, non-uniform lighting, and feature fusion from multiple sensor modalities to optimize performance in real-world autonomous driving scenarios.

ACKNOWLEDGEMENTS

The authors would like to express their gratitude to the test engineers of CARISSMA, Christoph Trost and Michael Graf, for their support in enabling the successful execution of the tests, and Dr. Dagmar Steinhauser for reviewing the dataset. The authors thank the Bayerisches Verbundforschungsprogramm (BayVFP) of the Freistaat Bavaria for funding the research project BARCS (DIK0351) in the funding line Digitization.

REFERENCES

Behret, V., Kushtanova, R., Fadl, I., Weber, S., Helmer, T., and Palme, F. (2025). Sensor Calibration and Data Analysis of the MuFoRa Dataset. Accepted at VISAPP 2025.

Bijelic, M., Gruber, T., Mannan, F., Kraus, F., Ritter, W., Dietmayer, K., and Heide, F. (2020). Seeing Through Fog Without Seeing Fog: Deep Multimodal Sensor Fusion in Unseen Adverse Weather. In *2020 IEEE/CVF Conference on Computer Vision and Pattern Recognition (CVPR)*, pages 11679–11689, Seattle, WA, USA. IEEE.

Burnett, K., Wu, Y., Yoon, D. J., Schoellig, A. P., and Barfoot, T. D. (2023). Are We Ready for Radar to Replace Lidar in All-Weather Mapping and Localization? arXiv:2203.10174 [cs].

Caesar, H., Bankiti, V., Lang, A. H., Vora, S., Liong, V. E., Xu, Q., Krishnan, A., Pan, Y., Baldan, G., and Beijbom, O. (2020). nuScenes: A multimodal dataset for autonomous driving. arXiv:1903.11027 [cs, stat].

Carion, N., Massa, F., Synnaeve, G., Usunier, N., Kirillov, A., and Zagoruyko, S. (2020). End-to-end object detection with transformers.

Cordts, M., Omran, M., Ramos, S., Rehfeld, T., Enzweiler, M., Benenson, R., Franke, U., Roth, S., and Schiele, B. (2016). The cityscapes dataset for semantic urban scene understanding.

Deng, J., Shi, S., Li, P., Zhou, W., Zhang, Y., and Li, H. (2021). Voxel R-CNN: Towards High Performance Voxel-based 3D Object Detection. arXiv:2012.15712 [cs].

El-Shair, Z. A., Abu-raddaha, A., Cofield, A., Alawneh, H., Aladem, M., Hamzeh, Y., and Rawashdeh, S. A. (2024). SID: Stereo image dataset for autonomous driving in adverse conditions.

Geiger, A., Lenz, P., Stiller, C., and Urtasun, R. (2013). Vision meets robotics: The KITTI dataset. *The International Journal of Robotics Research*, 32(11):1231–1237.

Graf, M., Vriesman, D., and Brandmeier, T. (2023). Testmethodik zur untersuchung, validierung und absicherung von störeinflüssen auf umfeldsensoren durch witterung unter reproduzierbaren bedingungen. *VDI Verlag*, abs/1405.0312.

Gultepe, I., Tardif, R., Michaelides, S. C., Cermak, J., Bott, A., Bendix, J., Müller, M. D., Pagowski, M., Hansen, B., Ellrod, G., Jacobs, W., Toth, G., and Cober, S. G. (2007). Fog Research: A Review of Past Achievements and Future Perspectives. *Pure and Applied Geophysics*, 164(6-7):1121–1159.

Heinzler, R., Schindler, P., Seekircher, J., Ritter, W., and Stork, W. (2019). *Weather Influence and Classification with Automotive Lidar Sensors*.

Hu, X., Fu, C.-W., Zhu, L., and Heng, P.-A. (2019). Depth-attentional features for single-image rain removal.

Jocher, G., Qiu, J., and Chaurasia, A. (2023). Ultralytics YOLO.

Jokela, M., Kutila, M., and Pyykönen, P. (2019). Testing and Validation of Automotive Point-Cloud Sensors in Adverse Weather Conditions. *Applied Sciences*, 9:2341.

Kenk, M. A. and Hassaballah, M. (2020). DAWN: Vehicle Detection in Adverse Weather Nature Dataset. arXiv:2008.05402 [cs].

Lakra, K. and Avishek, K. (2022). A review on factors influencing fog formation, classification, forecasting, detection and impacts. *Rendiconti Lincei. Scienze Fisiche e Naturali*, 33(2):319–353.

Liao, Y., Xie, J., and Geiger, A. (2022). KITTI-360: A Novel Dataset and Benchmarks for Urban Scene Understanding in 2D and 3D. arXiv:2109.13410 [cs].

Mao, J., Niu, M., Jiang, C., Liang, H., Chen, J., Liang, X., Li, Y., Ye, C., Zhang, W., Li, Z., Yu, J., Xu, H., and Xu, C. (2021). One Million Scenes for Autonomous Driving: ONCE Dataset. arXiv:2106.11037 [cs].

Marathe, A., Ramanan, D., Walambe, R., and Kotecha, K. (2023). WEDGE: A multi-weather autonomous driving dataset built from generative vision-language models. arXiv:2305.07528 [cs].

Miclea, R.-C., Dughir, C., Alexa, F., Sandru, F., and Silea, I. (2020). Laser and LIDAR in a System for Visibility Distance Estimation in Fog Conditions. *Sensors*, 20(21):6322.

Ros, G., Sellart, L., Materzynska, J., Vazquez, D., and Lopez, A. M. (2016). The SYNTHIA dataset: A large collection of synthetic images for semantic segmentation of urban scenes. In *2016 IEEE Conference on Computer Vision and Pattern Recognition (CVPR)*, pages 3234–3243. IEEE.

Sakaridis, C., Dai, D., and Van Gool, L. (2021). ACDC: The adverse conditions dataset with correspondences for semantic driving scene understanding. In *2021 IEEE/CVF International Conference on Computer Vision (ICCV)*, pages 10745–10755. IEEE.

Sezgin, F., Vriesman, D., Steinhauser, D., Lugner, R., and Brandmeier, T. (2023). Safe Autonomous Driving

in Adverse Weather: Sensor Evaluation and Performance Monitoring. arXiv:2305.01336 [cs].

SICK AG (2018). *Operating Instructions: VISIC620 Visibility Measuring Device*. SICK AG, 201.

Sun, P., Kretzschmar, H., Dotiwalla, X., Chouard, A., Patnaik, V., Tsui, P., Guo, J., Zhou, Y., Chai, Y., Caine, B., Vasudevan, V., Han, W., Ngiam, J., Zhao, H., Timofeev, A., Ettinger, S., Krivokon, M., Gao, A., Joshi, A., Zhang, Y., Shlens, J., Chen, Z., and Anguelov, D. (2020). Scalability in Perception for Autonomous Driving: Waymo Open Dataset. In *2020 IEEE/CVF Conference on Computer Vision and Pattern Recognition (CVPR)*, pages 2443–2451, Seattle, WA, USA. IEEE.

Vriesman, D., Thoresz, B., Steinhauser, D., Zimmer, A., Britto, A., and Brandmeier, T. (2020). An experimental analysis of rain interference on detection and ranging sensors. In *2020 IEEE 23rd International Conference on Intelligent Transportation Systems (ITSC)*, pages 1–5.

World Meteorological Organization (2008). *Guide to Meteorological Instruments and Methods of Observation*. WMO-No. 8. World Meteorological Organization, Geneva, seventh edition.

Yu, F., Chen, H., Wang, X., Xian, W., Chen, Y., Liu, F., Madhavan, V., and Darrell, T. (2020). BDD100k: A diverse driving dataset for heterogeneous multitask learning.

Zhang, C., Huang, Z., Guo, H., Qin, L., Ang, M. H., and Rus, D. (2023). SMART-Rain: A Degradation Evaluation Dataset for Autonomous Driving in Rain. *2023 IEEE/RSJ International Conference on Intelligent Robots and Systems (IROS)*, pages 9691–9698. Conference Name: 2023 IEEE/RSJ International Conference on Intelligent Robots and Systems (IROS) ISBN: 9781665491907 Place: Detroit, MI, USA Publisher: IEEE.

Zhou, Y. and Tuzel, O. (2017). VoxelNet: End-to-End Learning for Point Cloud Based 3D Object Detection. arXiv:1711.06396 [cs].

APPENDIX

Figure 7: From top to bottom: Target objects positioned 45 meters from the sensors in dry conditions, and positioned at 45, 35, 25, 15, and 5 meters respectively during the fog-visibility level of approx. 35 meters.

Table 4: Sensor positions (x y z) relative to the total station origin over the five test days.

Sensor	Day 1	Day 2	Day 3	Day 4	Day 5
Qb2 left	$\begin{pmatrix}37.84\\3.70\\1.66\end{pmatrix}$	$\begin{pmatrix}37.84\\3.72\\1.66\end{pmatrix}$	$\begin{pmatrix}37.78\\3.40\\1.66\end{pmatrix}$	$\begin{pmatrix}37.79\\3.38\\1.66\end{pmatrix}$	$\begin{pmatrix}37.76\\3.39\\1.66\end{pmatrix}$
Qb2 right	$\begin{pmatrix}37.80\\4.61\\1.66\end{pmatrix}$	$\begin{pmatrix}37.81\\4.62\\1.66\end{pmatrix}$	$\begin{pmatrix}37.79\\4.32\\1.66\end{pmatrix}$	$\begin{pmatrix}37.79\\4.29\\1.66\end{pmatrix}$	$\begin{pmatrix}37.77\\4.28\\1.66\end{pmatrix}$
ZED2i	$\begin{pmatrix}37.86\\4.08\\1.62\end{pmatrix}$	$\begin{pmatrix}37.85\\4.10\\1.62\end{pmatrix}$	$\begin{pmatrix}37.82\\3.79\\1.62\end{pmatrix}$	$\begin{pmatrix}37.82\\3.75\\1.62\end{pmatrix}$	$\begin{pmatrix}37.79\\3.75\\1.62\end{pmatrix}$

Figure 8: From top to bottom: Target objects positioned 15 meters from the sensors in dry conditions, and positioned at 15, 10, and 5 meters respectively during the fog-visibility level of approx. 8 meters.

Figure 9: From top to bottom: Target objects positioned 50 meters from the sensors in dry conditions, and during rain precipitation of 20, 60, and 100 mm/h.